ISO'S SHORT WAVELENGTH SPECTROMETER - ULTIMATE SENSITIVITY

Reducing the effects of cosmic weather

E.A. VALENTIJN
SRON, Kapteyn Institute, P.O. Box 800, 9700 AV Groningen, The Netherlands

AND

W.F. THI
Leiden Observatory, P.O. Box 9513, 2300 RA Leiden, The Netherlands

Abstract. Compared to the pre-launch measurements, the in-orbit noise levels of the Short Wavelength Spectrometer (SWS) detectors show a significant increase, considerably lowering the overall sensitivity. Cosmic ray impacts on the detectors and/or on the instrument electronics play an important role in the noise levels and consequently many observations of faint sources are affected by this increased noise. However, by taking advantage of the high read-out frequency of 24 Hz and the redundancies provided by the observing strategy, it is possible to significantly improve the quality of the data. Here, we present the concept of self-calibration and additional algorithms, which are successfully applied to recover the weak signals of molecular hydrogen lines undetectable in a standard data reduction.

1. Introduction

The SWS AOT2 grating observing mode (de Graauw et al. 1996) is designed to observe spectral lines and a small range of the surrounding continuum with a spectral resolution $\lambda/\Delta\lambda$ around 2000. Many observations are undertaken in this mode in order to detect weak lines with a sensitivity which is set by the noise level.

The SWS detectors have the ability to perform a non-destructive read-out, which means that the charge is not altered by sampling its current value (Leech et al. 1997, thereafter SWS IDUM). An exposure is controlled by sequences of resets and read-outs. The signal is sampled 24 times per second

and reset every 2 seconds. The slope of the Voltage increase within a reset interval, expressed in μV/s, is linearly related to the flux incident on the detectors (1 μV/s corresponds more or less to 1 Jy). In practice, the slope is obtained by best fitting the data points, which however are first corrected for the curvature (linearized) due to a high-pass filter (characterized by a RC time constant) and due to the after-effect of applying the reset pulse.
During the instrument level tests in the laboratory, we have obtained typical effective root mean square (r.m.s.) noise values for the 6 different types of the SWS detectors in the range 0.5 - 1.0 μV/s (Table 1). These data are determined for slopes with a reset interval of 2 seconds (48 data points). In orbit, similar dark current measurements have effective r.m.s. values which are considerably larger, even when the data is filtered with the standard pipeline de-glitcher (cf. column 4). The behavior depends on the type of material and is related to the dimensions of the detectors and hysteresis effects. For instance, for the small (120 $\times$120 μm) InSb diode-detectors, which hardly have any memory effects, the in-orbit increase of noise is small, while the larger (420 $\times$370 μm = dispersion $\times$ cross dispersion direction) Si:As BIBIB detectors exhibit noise figures ten times higher in space than during the laboratory tests. The large Ge:Be detectors (450 $\times$450 μm) also display memory effects. Both the detector noise characteristics and the dark current values are varying in time in a fashion which was not observed under laboratory conditions. Regarding these properties no two observations are identical, suggesting that we are sensing the, sometimes erratic, effects of space weather. Note that in particular the BIBIB elements can stay in a triggered state for various time scales, ranging from minutes, to hours and even weeks.

TABLE 1. **R.m.s. noise under dark conditions**

band	**material**	**lab. μV/s**	**in orbit μV/s**
1	**In:Sb**	**0.6**	**0.6 - 1.0**
2	**Si:Ga**	**0.6**	**1.5 - 3.5**
3	**Si:As BIBIB**	**0.5**	**4 - 5**
4	**Ge:Be**	**0.9**	**5 - 15**
5	**Si:Sb**	**0.5**	**2 - 6**
6	**Ge:Be**	**1.0**	**1.4 - 2**

In this paper, we describe various effects which tend to increase the noise level. The standard data processing is not able, at the moment, to handle these effects. In order to detect weak lines, we have developed dedicated data processing methods. We will introduce the concept of self-calibration,

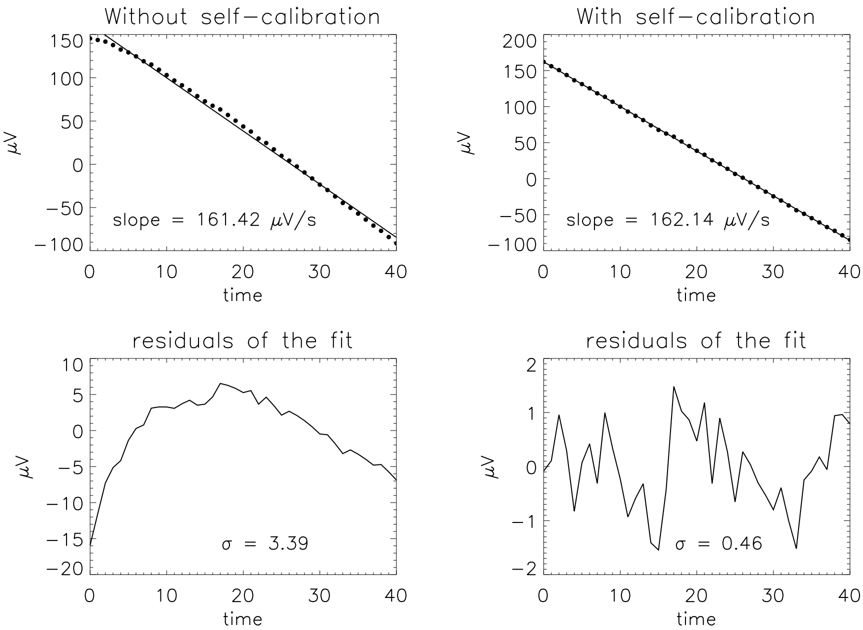

Figure 1. **An example of the effect of self-calibration on one ramp with a 2 second reset interval not affected by glitches. The upper plots show the fit of the data points (dots) by a straight line after correction for the shape of the after-reset pulse and the curvature introduced by a high-pass filter. The left fit is obtained without using self-calibration and the standard deviation is high ($\sigma = 3.39\mu$V/s). The right fit is performed after applying self-calibration. In that case the standard deviation is much better ($\sigma = 0.46\mu$V/s).**

which benefits from the high frequency readout (24 Hz) of the detectors and discuss various algorithms which take advantage of the redundancy of the data as set by the AOT observing strategy. For the development of our procedures we focussed on the, more or less hysteresis-free, BIBIB detectors; the code is also applicable to other detector materials, but is perhaps not fully optimized.

2. Causes of increased noise

The basic noise in the overall detector/amplifier chain, in dark conditions, and in an environment free of ionizing radiation, is caused by amplifier noise. We identify a variety of origins for an increase of this noise level.

i): First, there are *fluctuations of the level of the dark current.* For an AOT2 observation, the dark currents are measured before and after each up and down scan (i.e. every 200 s) during 10 resets. These dark currents

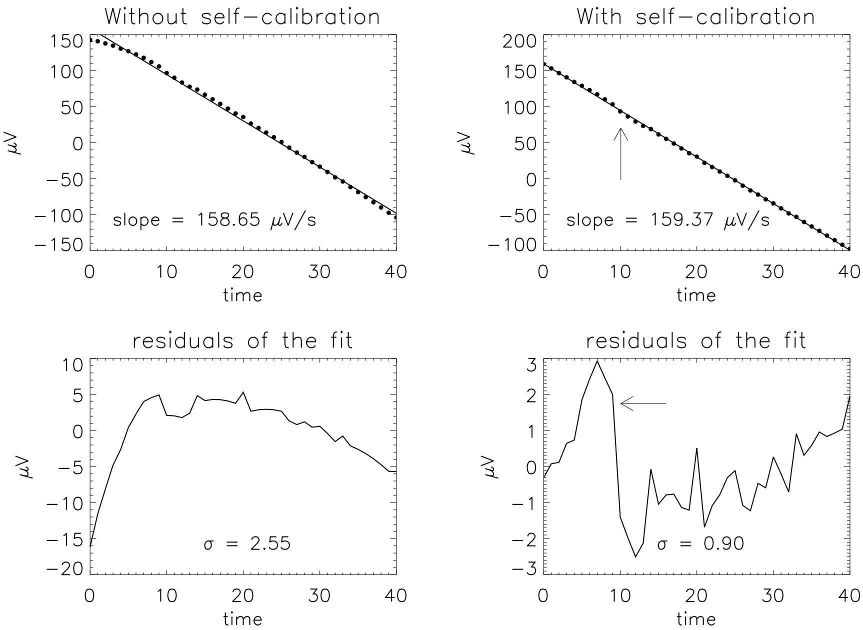

Figure 2. **These plots show the effect of a "mini-glitch" on the fit of the slope. The arrows indicate the position of the "mini-glitch". After application of the self-calibration, the standard deviation of the fit remains high (0.9 μV/s), so this "mini-glitch" will be detected by the filtering software.**

often show drifts on various time scales and sometimes sudden jumps of the mean level. The amplitudes of the variations could be as high as 10 μV/s, whereas we aim to observe a signal of about 1 μV/s or less. As well as the science data, the dark currents are affected by glitches, which are consequences of cosmic ray hits on the detectors. In order to properly model the long term variations of the dark current, the individual dark current measurements should be de-glitched as much as possible.

ii): We identify two kinds of glitches: *maxi-glitches* are those noted as small jumps in a series of slope determinations of the ramps (corresponding to both "spikes" = "big slope jumps" and "glitches" = "big ramp jumps" in Wieprecht at al. 1999) and *mini-glitches* which can only be noted as a *small* jump within a particular ramp. Maxi glitches are mostly tackled by the standard pipeline de-glitcher. Mini-glitches can be identified using the standard deviation of ramp-fits, provided that the ramp has been well linearized first (cf. Fig 1 and 2).

Whereas up to 30% of the data can be affected by mini-glitches, which are most likely caused by secondary electrons produced by a heavy particle im-

pact, the standard processing is designed to detect only the "maxi-glitches". The effect of a heavy impact could sometimes last for a few reset intervals: the large amount of electron-hole pairs generated by the particle's hit disappears only after a few resets and follows an exponential decay law. We attribute the name *glitch tails* to this phenomenon.
iii): Contrary to the laboratory situation, we detected in orbit events simultaneously on all the elements of a detector array, with a more or less comparable amplitude. We suspect that these *correlated events* are caused by electrical disturbances of the readout circuit due to ionizing radiation.
iv): Finally, the standard processing uses calibration files which describe properties of the electronics, such as electrical crosstalk, the after-reset pulse shape and the RC time constants. These characteristics were derived during the laboratory Instrumental Level Tests (SWS IDUM, chapter 8). It was originally expected that these characteristics would remain constant during the mission. The in-orbit performance shows that this assumption is not always fulfilled and the inadequacy of the calibration results in an increased noise in the final spectrum. Particularly, the after-reset pulse shapes of individual detector elements of the BIBIB array were found to vary significantly on at least an orbit to orbit time scale. The on-the-fly characterization of this variation is done in our *"self-calibration"* procedures.
Although it is suspected that these variations are caused by cosmic ray impacts, the actual process is not well understood.

3. Special data processing

In order to correct for the drifts of the electronic characteristics and to detect data affected by glitches, we developed software based on two concepts: adaptation of the calibration data to the science data and intense use of the redundancies.

3.1. SELF-CALIBRATION

The science data contain by itself information which can be used to derive its own calibration. The goal is to improve the linearization of the ramp, i.e. with a low standard deviation σ of the fit (cf. Fig. 1). This way, the standard deviation of the ramp fit becomes a reliable estimate of the quality of the data and will be used as a criterion by the subsequent mini-glitch filtering software (cf. Fig 2).
The two fluctuating characteristics deduced from the science data are the after-reset pulse shape and the RC time constant. First, the software finds the best values for the after-reset pulse shape from a sub-set of science data unaffected by glitches. Experiments showed that most of the variations in

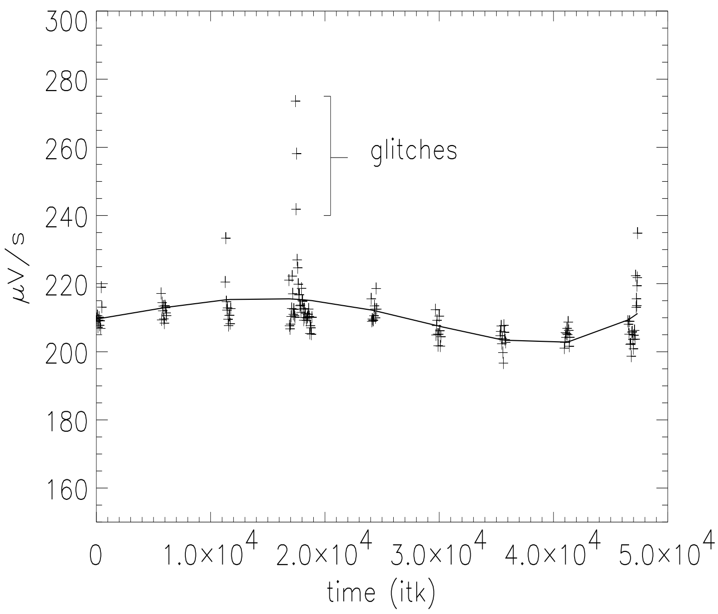

Figure 3. **Fit of the dark current measurements (represented by the cross) by a 4^{th} order polynomial (line). Notice that the dark current measurements could also be corrupted by glitches.**

the characteristics are due to fluctuations in the after-reset pulse shape, whose amplitude can vary up to a factor 3, while the variations on time constants are generally small. It is not excluded that the fine-tuning of the time constants in fact corresponds to remaining imperfections of the pulse shape determinations. For our purposes this discrimination does not matter.

The application of our updated calibration of pulse-shapes and time constants did not change the continuum level of our spectra by more than 10%. Thus our flux scale is not significantly affected by the particular changes of calibration parameters.

The present idea of self-calibration is also implemented in the SWS Interactive Analysis tool `derive_pulse shape`. After deriving these calibration data the raw data are processed with the standard pipeline and the Standard Processed Data (SPD) are obtained.

The next stage consists of the dark current subtraction using a polynomial (1-7 order) interpolation of measurements not affected by glitches. The aim is to correct the dark drifts and sudden jumps (cf. Fig 3).

The comparison between the up and down scan can be used for the detection of glitch tails which exhibit a low standard deviation and are not detected by the above algorithm. This procedure is applied essentially when we possess only one scan up and one scan down. In that case, a simple statistical average of data in each spectral bin to determine the observed flux will be biased by glitch tails. This results in a continuum showing artificial oscillations. We designed an algorithm to correct this bias. The principle is to compare the fluxes obtained by each scan individually. All differences could be related to noises, drifts or the glitch tails. We illustrate the effect of removing a glitch tail on the final result in Fig 4. The mean of the data corresponding to each wavelength bin (i.e. the oversampling) is computed separately for the up and down scan ($\mathrm{m_{up}}(\lambda)$ and $\mathrm{m_{down}}(\lambda)$). Then we store in the vector $\Delta\mathrm{m}(\lambda)$ the difference between the up and the down scan. Then the mean $<\Delta\mathrm{m}(\lambda)>$ and the standard deviation $\sigma(\Delta\mathrm{m}(\lambda))$ is calculated. Without bias, $<\Delta\mathrm{m}(\lambda)>$ and σ $(\Delta\mathrm{m}(\lambda))$ tend to zero with decreasing noise level. If a glitch tail occurs at λ_o during the up scan, the value $\mathrm{m_{up}}(\lambda_o)$ is much higher than $\mathrm{m_{down}}(\lambda_o)$, then $|\ \Delta\mathrm{m}(\lambda_o)|$ lies outside the range $<\Delta\mathrm{m}(\lambda)> + \ \sigma(\Delta\mathrm{m}(\lambda))$ and vice versa. The bigger value of $\mathrm{m_{up}}(\lambda)$ and $\mathrm{m_{down}}(\lambda)$ is assigned a weight inversely proportional to its deviation to the mean difference between the two scans $\mathrm{w_{up\ or\ down}}(\lambda_\mathrm{o}) =|\ \mathrm{m_{up\ or\ down}}(\lambda_\mathrm{o}) - <\Delta\mathrm{m}(\lambda)>|$, and we assign a weight of unity to the other mean. This weight is used when we recombine all the data. When lots of scans are available, the median is able to remove the effects of glitch tails and there is no strong need of an up-down scan correction.

The responsivity and photometric calibrations are done using the standard data processing method.

Finally, our filtering and analysis program performs various filterings: a *drift filter* minimizes unaccounted drifts in dark current and responsivities of individual detector elements. In fact, this process could be used to fully replace the dark current subtraction. In this step the input data, still ordered in time with up-down wavelength scanning, are smoothed with a low frequency filter, and the result is subsequently subtracted from the original data. Note that the observational data of a SWS AOT2 spectrum can contain many up-down scans. Clearly, information about the continuum is lost this way, but here we are interested in maximizing the signal to noise ratio of a spectral line. The value of the continuum can be determined by running the software with the drift filter switched off. Data flagged as glitches (max-

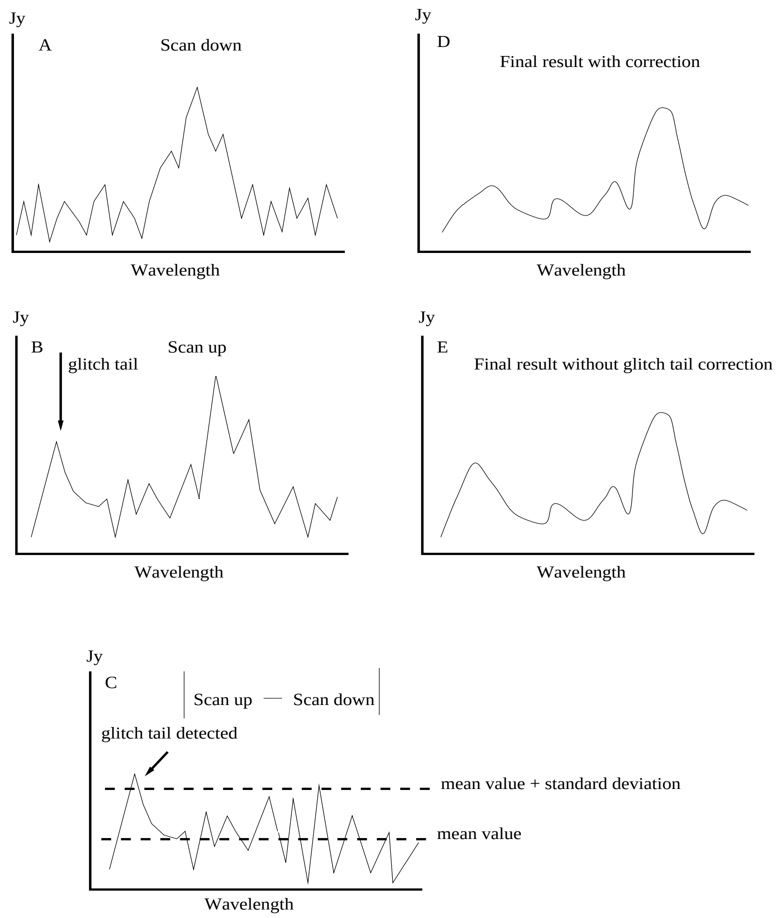

Figure 4. **A schematic illustration of the effect of applying the up-down scan correction on the final result. Plots A and B are the final result obtained respectively with only the down and the up scan data. In plot C, the glitch tail is detected due to his higher flux. Plots D and E show the difference between final spectrum obtained with and without applying the glitch tail correction.**

imum flux threshold for maxi-glitches, maximum σ value for mini-glitches) are discarded (cf. Fig 5). Noise components which appear simultaneously in a few detectors (correlated events) are optionally filtered by subtracting for each detector element the mean signal of all other detector elements of the array.

The software makes an analysis of the data, computing some statistic values such as the noise level or the number of “bad” data values.

Our procedures are highly interactive, and the user is required to respon-

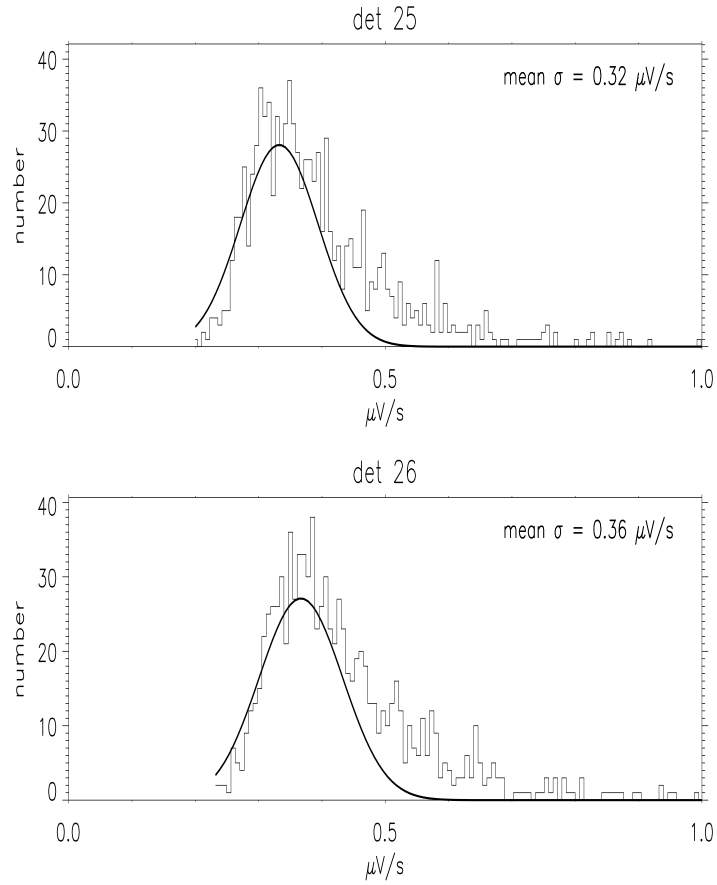

Figure 5. **Standard deviation distribution for detector 25 and 26. The line represents a fit with a Gaussian distribution. The tail of data points with a high standard deviation is caused by mini-glitches and these can be filtered in the reduction of the spectra.**

sibly fine-tune and verify the applied filter values e.g.:

- tuning the clipping of large slope values after inspecting the possibly brightest line in the spectrum,
- not filtering extended lines by applying too narrow drift filters, or the correlated noise filter,
- not decreasing the S/N by clipping too many data points by accepting only too low standard deviations of ramps fits,
- selecting the best set of detectors of the array on the basis of the noise and offset level characteristics of the various detector elements.

In judging the end result, the user will have to evaluate the stability of the result for the chosen filter values. This way, the code can also be used to verify the credibility of detected lines reduced with other algorithms.

3.3. PERFORMANCE OF THE SPECIAL PROCESSING

In Table 2 we present the r.m.s. of the slopes of individual band 3 detector elements at various stages of the filtering process (revolution 132 data). We notice that two detectors (29 and 34) were so "damaged" by cosmic ray events that their dark current was significantly increased, preventing also our method to become effective. In the end result, the number of data points is decreased by 25 - 30% and the noise level decreases by a factor of 3 in general. The values given in column 2, for MAXI-deglitching ON and all other filters OFF, correspond closely to those obtained from the standard pipeline (cf Table 1, column 4) with active de-glitcher, which essentially filters the same data points as labeled maxi-glitch by our code. The frequency of maxi-glitches is an order of magnitude less than that of the mini-glitches.

TABLE 2. **R.m.s. (μV/s) at different stage of the data processing. SELF -CAL : self-calibration, DRIFT : drift correction, MINI : mini-glitches discarded, MAXI: maxi-glitches discarded, /cor : correlated events removed, /next : glitch-tails removed**

Det.	NO SELF-CAL NO DRIFT NO MINI MAXI	SELF-CAL NO DRIFT NO MINI MAXI	SELF-CAL DRIFT NO MINI MAXI	SELF-CAL DRIFT MINI MAXI	SELF-CAL DRIFT MINI MAXI /cor	SELF-CAL DRIFT MINI MAXI /cor /next
25	6.04	5.38	4.69	2.75	2.15	2.05
26	12.77	5.88	5.35	2.51	1.45	1.33
27	8.02	5.77	5.23	2.37	1.60	1.33
28	7.37	6.98	6.65	3.17	2.25	2.19
29	*12.41*	*11.25*	*10.30*	*9.18*	-	-
30	6.40	10.37	9.70	3.61	3.15	2.88
31	5.80	5.65	5.00	2.98	1.90	1.85
32	5.76	5.75	5.32	2.89	1.82	1.72
33	4.91	5.42	5.10	2.68	1.70	1.68
34	*75.39*	*75.95*	*59.7*	*61.93*	-	-
35	4.74	5.23	4.89	2.38	1.65	1.52
36	4.76	4.90	4.56	2.37	1.75	1.62

3.4. SCIENCE OBSERVATIONS

A sample of the photo-dissociation region IC 63 spectra (Thi et al. 1997) is presented in Fig 6. The observations were carried out using the ISO-SWS02 mode and typical observing times were 200-400 s per line. Using our specific method, two pure-rotational molecular hydrogen lines (S(1) at 17.035 μm and S(0) at 28.219 μm) as weak as 0.5 Jy can be detected in band 3 after subtraction of the continuum. Further results are presented in Valentijn & van der Werf (1999), Thi et al. (1999, a, b).

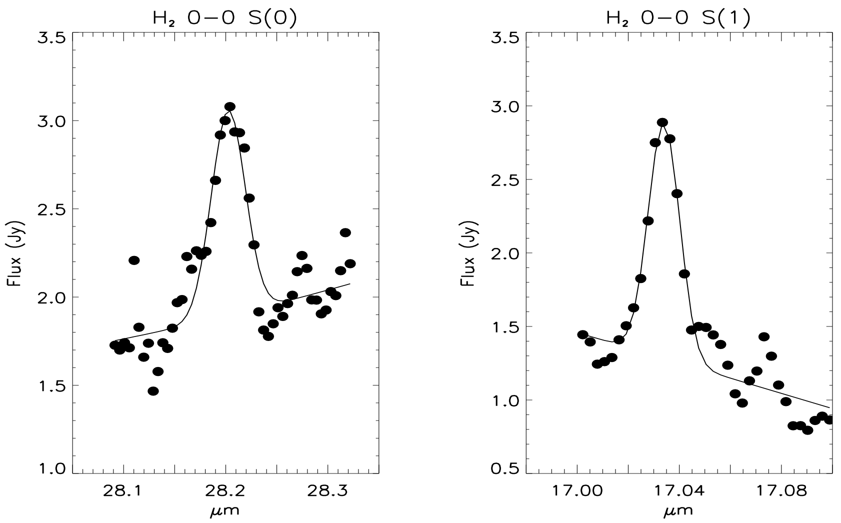

Figure 6. **ISO-SWS02 observations of H_2 lines toward IC 63. (Thi et al. 1997)**

4. Conclusion and further prospects

By applying self-calibration and using software which takes advantage of the redundancy and high-frequency read-out, we are able to correct partially for the diminished sensitivity of the SWS detectors, which is mostly due to the effects of the cosmic rays near the basic noise level. Each observation is unique and only the self-calibration can manage the variations of the instrument characteristics on a short time scale (on the order of 1 hour). The user fine-tunes dedicated filters to further optimize and verify the result.
In the end result, the noise distribution in the spectra is nearly Gaussian, and the tail with high standard deviations of the ramp fits is cut out (cf. Fig 5). We believe, these procedures optimally filter the various effects of the cosmic weather. A next step could be to restore skipped data points leading to at most a 15% improvement in overall r.m.s. A more fundamental improvement could be the inclusion of the tweaking of the electrical crosstalk matrix in our self-calibration procedures, which might improve

the correction for correlated events. A user-friendly version of our method has been implemented in the SWS IA package.

References

de Graauw Th. et al. 1996, Observing with ISO Short-Wavelength Spectrometer, *A&A* **315, L49**

Leech K. et al. 1997, SWS Instrument Data Users Manual, Issue 3.1, SAI/95-221/Dc

Thi W.F, van Dishoeck E.F. et al., 1997, Weak H_2 emission from translucent clouds, Proceedings of the First ISO Workshop on Analytical Spectroscopy, Madrid, 6-8 Oct 1997, p. 299-300

Thi, W.F, van Dishoeck, E.F. et al., 1999a, H_2 emission from disks around Herbig Ae and T Tauri stars, in The Universe as seen by ISO, Eds P.Cox, M.F. Kessler, ESA - SP-427

Thi, W.F, van Dishoeck, E.F., Black, J.H., Jansen, D.J, Evans, N.J., Jaffe, D.T., 1999b, Weak H_2 emission from diffuse and translucent clouds, in The Universe as seen by ISO, Eds P.Cox, M.F. Kessler, ESA - SP-427

Valentijn, E.A. & van der Werf, P.P., 1999, The ISO-SWS survey for molecular hydrogen in galaxies, in The Universe as seen by ISO, Eds P.Cox, M.F. Kessler, ESA - SP-427

Wieprecht E., Wiezorrek E. et al., 1999, SWS-Detector Glitch effect corrections, this proceedings